Structural and thermodynamic properties of liquid Na-Li and Ca-Li alloys at high pressure

A. M. Teweldeberhan[1] and S. A. Bonev[1,2]
[1]*Lawrence Livermore National Laboratory, Livermore, California 94550, USA*
[2]*Department of Physics, Dalhousie University, Halifax, Nova Scotia B3H 3J5, Canada*
(Received 29 December 2010; published 20 April 2011)

The thermodynamic, electronic, and structural properties of liquid Na-Li and Ca-Li alloys at high pressure have been studied using *ab initio* molecular dynamics simulations. Gibbs free energies of pure Na, Ca, Li, and their mixtures (Na-Li and Ca-Li) are computed from vibrational density of states to determine the mixing-demixing behavior of the alloys. The computed electronic and structural properties of the mixtures with different concentrations are compared with the pure liquids up to around 265 GPa and 2000 K.

DOI: 10.1103/PhysRevB.83.134120 PACS number(s): 62.50.−p, 61.20.Ja, 71.15.Mb

I. INTRODUCTION

The electronic and structural properties of elemental alkali and alkaline-earth liquids under pressure have been extensively studied.[1–10] Electronic transitions characterized by *s*-to-*p* or *s*-to-*d* transfer and related appearance of structures with less compact local order have been predicted for Li, Na, and Ca liquids from first-principles calculations.[3,4,7] These changes are responsible for a number of interesting properties in Na and Li, including melting anomalies, pseudogap opening at temperatures as high as 1000 K, and dramatic lowering in conductivity.[1–4,6,11–16] A close analogy could be established between the solid and liquid phases of these elements. Thus, knowledge of liquid properties can provide insight into the properties of solids. An example for this is Li, where the existence of tetrahedral solid phases was suggested[4] based on molecular dynamics simulations of the liquid at 1000 K and later confirmed in a 0 K crystalline stability search.[17]

Little is known about the alkali and alkaline-earth liquid alloys. Although the electronic and structural properties of Na-Li mixtures at ambient pressure have been studied[18–21] using first-principles molecular dynamics (FPMD), high-pressure theoretical and experimental studies are scarce. Important open questions include the miscibility of such alloys under pressure and whether they exhibit symmetry-breaking changes in their local order similar to that found in the pure elements. In this paper, we compute the thermodynamic, structural, and electronic properties of Na-Li and Ca-Li liquid alloys at high pressure for several mixing concentrations and compare them with the pure liquids.

One of the difficulties in studying liquid mixtures is obtaining thermodynamic information from first principles. Previous studies[18–21] used partial pair correlation functions and structure factors to predict the phase separation tendency in Na-Li liquid alloy. Here, in addition to structural properties, we compute the Gibbs free energies of pure Na, Li, and Ca liquids as well as their mixtures using FPMD. In order to cover a large pressure-temperature-composition phase space, we have adopted an approximate method for computing liquid entropies. Details of the method are given Sec. II. In Sec III, we present and discuss the results and compare them with available experimental data. Sec. IV summarizes our findings.

II. COMPUTATIONAL DETAILS

The entropy of harmonic systems can be computed exactly from the vibrational density of states (VDOS). Even for strongly anharmonic systems, VDOS obtained from finite-temperature molecular dynamics simulations can be integrated to obtain a good first approximation to the free energy.[22] However, computation of liquid entropy from VDOS is problematic because of the finite value of the VDOS at zero frequency associated with diffusion. To circumvent the problem, Lin *et al.*[23] proposed to decompose the density of states of the liquid into a gas- and solid-like components. The idea is that the latter can be treated as harmonic oscillations, while for the former one has to introduce an approximate physical model.

In Ref. 23, the method is tested with classical potentials for a monatomic system at ambient pressure. The liquid VDOS is given by

$$D^l(\nu) = D^s(\nu) + D^g(\nu), \tag{1}$$

where $D^s(\nu)$ and $D^g(\nu)$ are the VDOS of the solid- and gas-like components, respectively. The gas-like component is computed from a hard-sphere model using

$$D^g(\nu) = \frac{D_0}{1 + \left(\frac{\pi D_0 \nu}{6 f N}\right)^2}. \tag{2}$$

Here D_0 is the VDOS of the liquid at zero frequency, N is the number of atoms, f is a fluidity factor obtained from

$$2\Delta^{-\frac{9}{2}} f^{\frac{15}{2}} - 6\Delta^{-3} f^5 - \Delta^{-\frac{3}{2}} f^{\frac{7}{2}} + 6\Delta^{-\frac{3}{2}} f^{\frac{5}{2}} + 2f - 2 = 0, \tag{3}$$

and Δ is a diffusivity constant given by

$$\Delta = \frac{2D_0}{9N}\left(\frac{\pi k_B T}{m}\right)^{1/2}\left(\frac{N}{V}\right)^{1/3}\left(\frac{6}{\pi}\right)^{2/3}. \tag{4}$$

The model has a single parameter, D_0, which is calculated from FPMD, after which Eqs. (3) and (4) are solved for the fluidity factor entering Eq. (2). Once D_0, f, and Δ are determined, the entropy of the liquid is computed as

$$S = k_B \int_0^\infty d\nu [D^s(\nu) W^s(\nu) + D^g(\nu) W^g(\nu)], \tag{5}$$

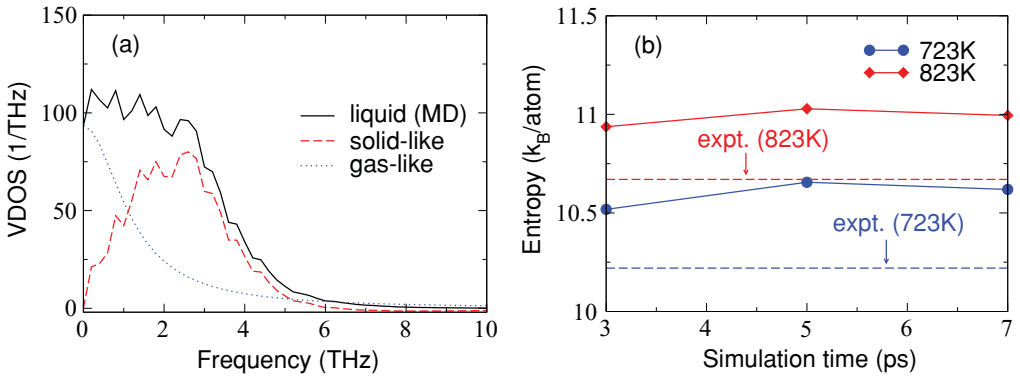

FIG. 1. (Color online) (a) VDOS of liquid Na at 723 K decomposed into solid- and gas-like components and (b) calculated entropies of liquid Na at 723 K (solid circles) and 823 K (solid diamonds) compared with experimental values from Ref. 34.

where W^s and W^g are weighing functions of the solid- and gas-like components given by

$$W^s(\nu) = \frac{\beta h\nu}{\exp(\beta h\nu) - 1} - \ln[1 - \exp(-\beta h\nu)], \qquad (6)$$

and

$$W^g(\nu) = \frac{1}{3}\left[\frac{S^{\mathrm{IG}}}{k_B} + \ln\left(\frac{1 + fy + f^2y^2 - f^3y^3}{(1 - fy)^3}\right) + \frac{fy(3fy - 4)}{(1 - fy)^2}\right]. \qquad (7)$$

Here $y = (f/\Delta)^{3/2}$ is the packing fraction, and S^{IG} is the entropy of an ideal gas.

The accuracy of this method is mostly dependent on the model used to separate the VDOS into gas- and solid-like components and the computation of the entropy contribution from the gas-like part. With the above hard-sphere model, it is reasonable to expect the liquid entropy to be overestimated. However, for monatomic systems under compression, the quantity D_0 decreases with pressure and the errors originating from adopting an ideal hard-sphere model are expected to decrease.

For more complex, multicomponent systems, there is no universal approach to define the gas-like component. The

TABLE I. Enthalpies H, Gibbs free energies G, and ionic entropies S of Na, Li, Ca, Na_xLi_{1-x}, and Ca_xLi_{1-x} for various concentrations x and pressures P. The enthalpies and Gibbs free energies are in eV/atom, pressures are in GPa, entropies are in k_B/atom, the ionic number densities ρ are in Å^{-3}. The electronic entropies are included in the enthalpy values and are of the order of $\sim 10^{-3}$ and $\sim 10^{-2}\, k_B$/atom at 1000 and 2000 K.

Na_xLi_{1-x} at 1000 K													
x	P	ρ_{NaLi}	ρ_{Na}	ρ_{Li}	H_{NaLi}	G_{NaLi}	S_{NaLi}	H_{Na}	G_{Na}	S_{Na}	H_{Li}	G_{Li}	S_{Li}
0.39	1.58	0.03762	0.02647	0.04773	−1.052	−1.850	9.260	−0.630	−1.565	10.850	−1.363	−2.066	8.158
	22.38	0.07191	0.05465	0.08891	1.181	0.518	7.694	2.309	1.533	9.005	0.403	−0.187	6.847
	41.73	0.08925	0.06806	0.11111	2.670	2.033	7.392	4.251	3.497	8.750	1.591	1.031	6.498
	79.38	0.11397	0.08661	0.14286	4.922	4.328	6.893	7.226	6.545	7.903	3.376	2.850	6.104
	97.81	0.12368	0.09337	0.15552	5.878	5.301	6.696	8.502	7.831	7.787	4.127	3.621	5.872
0.50	1.67	0.03546	0.02667	0.04808	−0.957	−1.789	9.655	−0.614	−1.547	10.827	−1.353	−2.054	8.135
	22.68	0.06831	0.05490	0.08930	1.420	0.740	7.891	2.342	1.569	8.970	0.423	−0.165	6.823
	42.46	0.08480	0.06850	0.11185	3.016	2.359	7.624	4.317	3.564	8.738	1.631	1.074	6.464
	79.94	0.10811	0.08682	0.14326	5.372	4.768	7.009	7.266	6.587	7.879	3.399	2.874	6.092
	98.61	0.11726	0.09370	0.15614	6.404	5.813	6.858	8.566	7.896	7.775	4.164	3.659	5.860
0.75	1.73	0.03107	0.02680	0.04831	−0.769	−1.652	10.247	−0.603	−1.535	10.815	−1.346	−2.046	8.123
	22.71	0.06097	0.05492	0.08934	1.894	1.164	8.471	2.345	1.573	8.959	0.425	−0.162	6.812
	42.52	0.07573	0.06853	0.11192	3.681	2.969	8.262	4.322	3.569	8.738	1.634	1.077	6.464
	79.82	0.09621	0.08676	0.14314	6.319	5.672	7.508	7.254	6.575	7.879	3.393	2.867	6.104
	98.77	0.10425	0.09378	0.15628	7.506	6.873	7.346	8.581	7.911	7.775	4.173	3.668	5.860
	145.31	0.12106	0.10825	0.18369	10.084	9.478	7.032	11.465	10.803	7.682	5.851	5.381	5.454
Ca_xLi_{1-x} at 2000 K													
x	P	ρ_{CaLi}	ρ_{Ca}	ρ_{Li}	H_{CaLi}	G_{CaLi}	S_{CaLi}	H_{Ca}	G_{Ca}	S_{Ca}	H_{Li}	G_{Li}	S_{Li}
0.50	3	0.03350	0.02526	0.05541	−0.767	−2.707	11.256	−0.533	−2.601	11.999	−0.981	−2.670	9.800
	267	0.15671	0.11584	0.23770	15.483	14.209	7.392	21.024	19.692	7.729	9.690	8.496	6.928

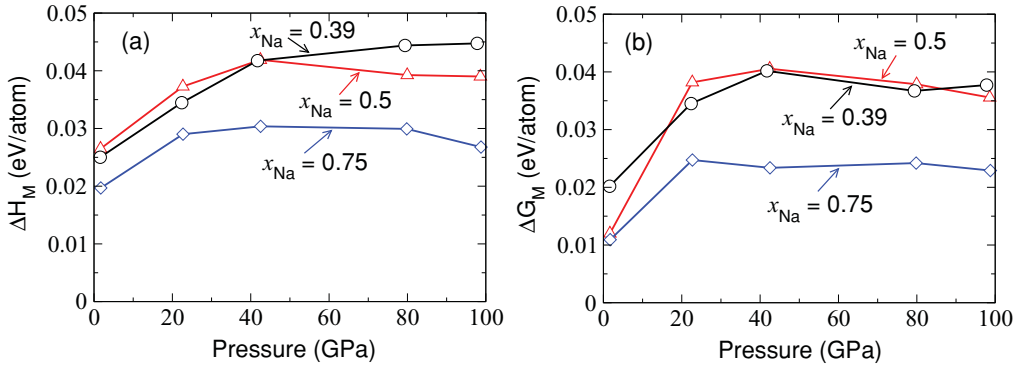

FIG. 2. (Color online) (a) Enthalpy and (b) Gibbs free energy of mixing of Na-Li liquid alloy at 1000 K for different Na concentrations (39%, 50%, and 75%).

model that is used must account for the particular physics of the system. Lin *et al.*[24] partitioned the VDOS of molecular H_2O into rotational, vibrational, and translational components to compute its entropy at ambient pressure. Since we do not have covalent bonding and the formation of molecules, the approach that we use here is different. We use the partial VDOS of Na, Ca, and Li atoms in the Na-Li and Ca-Li alloys to compute the entropies of the alloys.

The partial VDOS of each atomic species in the alloy is given by

$$D_\alpha^l(\nu) = x_\alpha \int_0^\tau C_\alpha(t)\cos(2\pi\nu t)dt, \tag{8}$$

where τ is the total simulation time after equilibration, x_α is the concentration of species α, and $C_\alpha(t)$ is the normalized velocity autocorrelation function

$$C_\alpha(t) = \frac{\left\langle \sum_{i_\alpha=1}^{N_\alpha} \mathbf{v}_{i_\alpha}(t)\cdot\mathbf{v}_{i_\alpha}(0)\right\rangle}{\left\langle \sum_{i_\alpha=1}^{N_\alpha} \mathbf{v}_{i_\alpha}(0)\cdot\mathbf{v}_{i_\alpha}(0)\right\rangle}. \tag{9}$$

Here $\mathbf{v}_{i_\alpha}$ is the velocity of atom i_α. The entropy of the alloy is then calculated according to

$$S = k_B \int_0^\infty d\nu \left[D^s(\nu)W^s(\nu) + \sum_\alpha D_\alpha^g(\nu)W_\alpha^g(\nu)\right], \tag{10}$$

with D_α^g and W_α^g determined for each species from Eqs. (2), (3), (4), and (7). The solid VDOS is defined as $D^s(\nu) = \sum_\alpha [D_\alpha^l(\nu) - D_\alpha^g(\nu)]$.

In order to determine the thermodynamic stability of Na-Li and Ca-Li alloys, their Gibbs free energy of mixing is calculated using

$$\Delta G_M = \Delta H_M - T\Delta S_M, \tag{11}$$

where the enthalpy (ΔH_M) and entropy (ΔS_M) of mixing are given by

$$\Delta H_M = H_{\mathrm{Na(Ca)Li}} - xH_{\mathrm{Na(Ca)}} - (1-x)H_{\mathrm{Li}} \tag{12}$$

and

$$\Delta S_M = S_{\mathrm{Na(Ca)Li}} - xS_{\mathrm{Na(Ca)}} - (1-x)S_{\mathrm{Li}}. \tag{13}$$

Here x represents the concentration of Na or Ca. The Gibbs free energy, $G = \langle U\rangle + \langle P\rangle V - \langle T\rangle S$, of the pure systems (Na, Ca, and Li) and their mixtures (Na-Li and Ca-Li) is computed under fixed number of atoms N, volume V, and temperature T from MD simulations as follows: $\langle U\rangle = \langle E\rangle + \langle KE\rangle$ is the sum of the Kohn-Sham energy and the kinetic energy of the ions, $P = -dE/dV + Nk_BT/V$, and $\langle ...\rangle$ represents the ensemble (time) average.

The FPMD simulations were carried out using the VASP code[25,26] in a canonical ensemble on cubic supercells

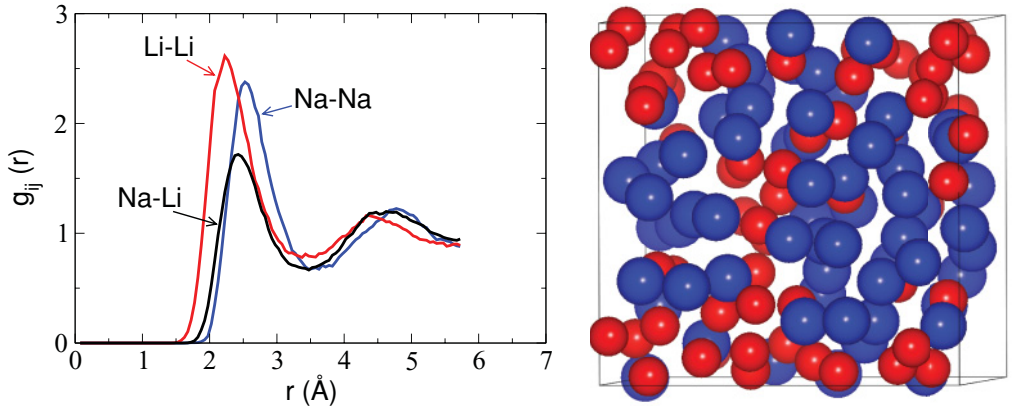

FIG. 3. (Color online) Partial pair correlation functions of Na-Na, Li-Li, and Na-Li in $Na_{0.5}Li_{0.5}$ liquid alloy at 42.5 GPa and 1000 K, and a snapshot of the atomic configuration from MD. The blue and red balls represent Na and Li atoms, respectively.

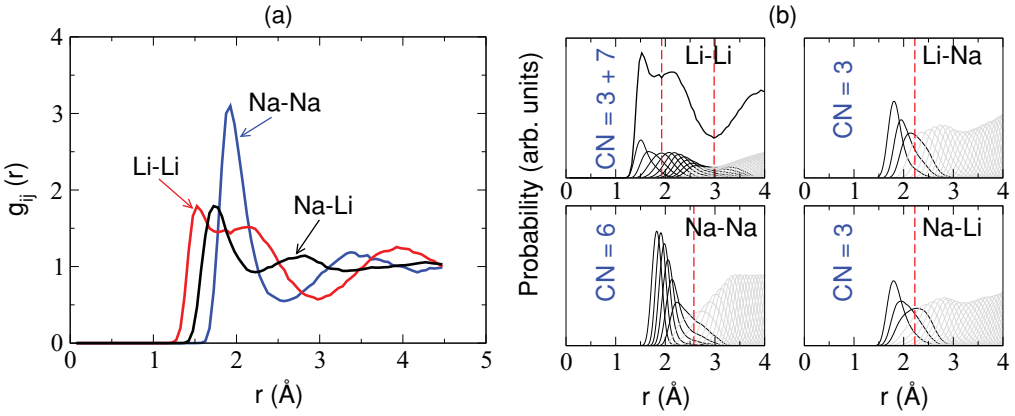

FIG. 4. (Color online) Partial pair correlation functions of Na-Na, Li-Li, and Na-Li in $Na_{0.5}Li_{0.5}$ liquid alloy at 264 GPa and 1000 K and histograms of nearest-neighbor distributions with their coordination numbers.

consisting 128 atoms (108 atoms are used for pure Ca). The calculations were performed with seven-, three-, and ten-electron projector augmented wave pseudopotentials[27,28] for Na, Li, and Ca, respectively, and the PW91-GGA parametrization[29,30] for the exchange-correlation functional. A plane-wave cutoff of 300 eV for Na, 272 eV for Li, and 290 eV for Ca have been used. We have used a nine-electron Na pseudopotential above 45 GPa with plane-wave cutoff of 700 eV for Na, Li, and their mixture. The equations of motion were integrated with ionic time steps of 1 fs, the Brillouin zone was sampled at the Γ point, and the ionic temperature was controlled with a Nosé-Hoover thermostat.[31,32] The initial structures (structures with randomly arranged atoms for the mixtures) were allowed to equilibrate for 3 ps at various temperatures and pressures for different concentrations. The simulations were then carried out for 5 ps to gather statistical information. To ensure convergence of the entropy, selected runs were performed for 7 ps after equilibration. The electronic densities of states were calculated with a $6 \times 6 \times 6$ Monkhorst-Pack mesh.[33]

III. RESULTS AND DISCUSSION

A. Entropy of liquid Na

To verify the accuracy of the method for computing liquid free energy, we start by calculating the entropy of liquid Na. The VDOS of liquid Na at 723 K decomposed into solid- and gas-like components and the entropy at 723 K and 823 K as a function of simulation time after equilibration are shown in Figs. 1(a) and 1(b). The results from the 5 and 7 ps simulations indicate that the 5 ps simulation is well converged and the entropies are in good agreement with the experimental values from Ref. 34. The calculations slightly overestimate the entropy, which is reasonable given the fact that the method assumes a hard-sphere model for the gas-like contribution. The calculated values are 3%–4% higher than the measured values. As discussed before, we expect the accuracy of the method to improve with pressure. Also, there should be cancellation of errors when calculating free energies of mixing because the structural properties of most of the systems considered here are similar.

B. Structural and thermodynamic properties of Na-Li alloy

The enthalpies, entropies, and Gibbs free energies of pure Na and Li and their mixtures at 1000 K are tabulated in Table I. The enthalpy and Gibbs free energy of mixing of the alloy as functions of pressure for different Na concentrations are shown in Figs. 2(a) and 2(b), respectively. We find a positive free energy of mixing up to around 100 GPa, indicating that the Na-Li alloy, which is a typical phase separating alloy at ambient pressure, exhibits a demixing behavior even

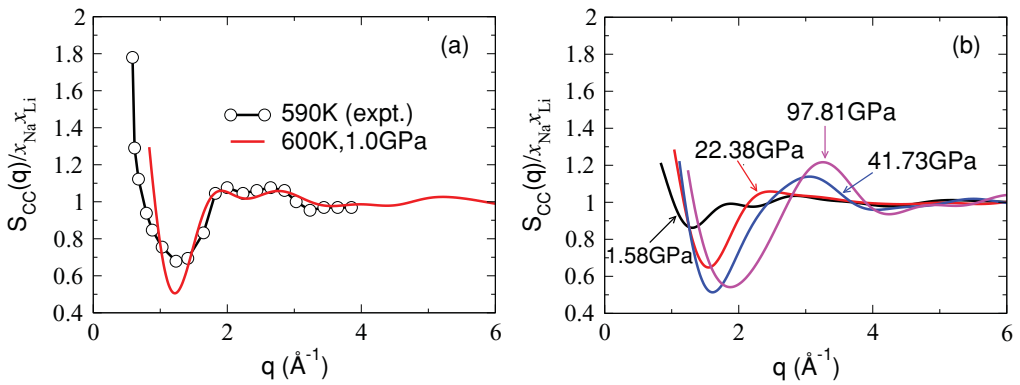

FIG. 5. (Color online) Calculated concentration-concentration structure factor, $S_{CC}(q)$, of $Na_{0.39}Li_{0.61}$ alloy (a) at 600 K together with experimental data at 590 K taken from Ref. 35, and (b) at 1000 K for different pressures.

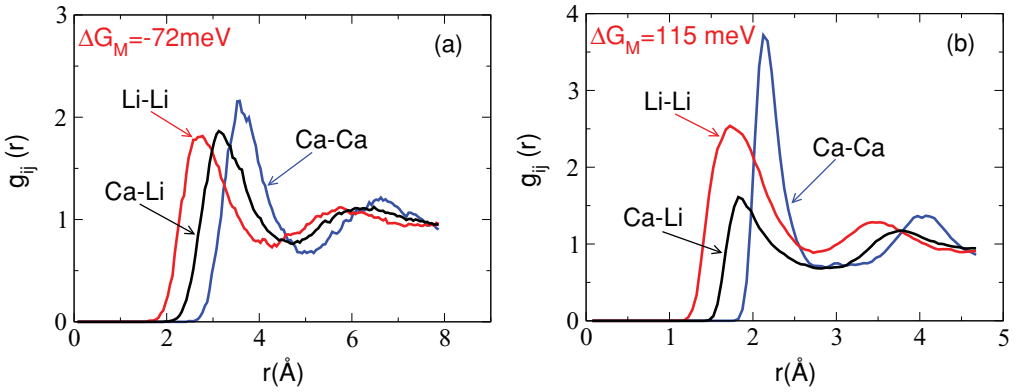

FIG. 6. (Color online) Partial pair correlation functions of Ca-Ca, Li-Li, and Ca-Li in $Ca_{0.5}Li_{0.5}$ liquid alloy at (a) 3 and (b) 267 GPa and 2000 K.

under compression. Compared to the lower Na concentrations, ΔG_M decreases for 75% Na, indicating a possible tendency of mixing. It stays positive and increases at higher pressure (30.5 meV/atom at 145.3 GPa). Nevertheless, the results indicate that the region below 100 GPa may be interesting for exploring stable Na-Li solids with large Na concentration.

The phase separation tendency can also be estimated from the partial pair correlation functions.[19] The partial pair correlation functions of $Na_{0.5}Li_{0.5}$ at around 40 GPa and 1000 K, which has a maximum Gibbs free energy of mixing, and the snapshot of the atomic configuration from MD are shown in Fig. 3. The first-peak heights of $g_{NaNa}(r)$ and $g_{LiLi}(r)$ are larger than $g_{NaLi}(r)$, indicating a tendency of homocoordination in the alloy. To estimate the phase separation behavior at high pressure, we computed the partial pair correlation functions of $Na_{0.5}Li_{0.5}$ at 264 GPa and 1000 K. The pair correlation functions are shown in Fig. 4(a). It is not obvious to predict the phase separation tendency from the first-peak heights of the pair correlation functions in this case because of the broadening and splitting of the Li-Li pair correlation function. The broadening and splitting behavior is also observed in pure Li.[4] Our coordination number (CN) analysis from histograms of nearest-neighbor distributions shown in Fig. 4(b) shows that the Na-Li CN is reduced compared to Na-Na or Li-Li, which indicates that the alloy exhibits a demixing behavior at high pressure.

Another way of looking at the phase separation is to compute the concentration-concentration (CC) structure factor of the alloy which is given by[19]

$$S_{CC}(q) = x_{Na}x_{Li}[x_{Na}S_{LiLi}(q) + x_{Li}S_{NaNa}(q) - 2(x_{Na}x_{Li})^{1/2}S_{NaLi}(q)], \quad (14)$$

where S_{ij} are partial structure factors obtained by Fourier-transforming the partial pair correlation functions and x_i is the concentration of atom i. The CC structure factor of a phase-separating alloy diverges in the long-wavelength limit. The computed structure factor for the $Na_{0.39}Li_{0.61}$ alloy at 600 K together with experimental data[35] at 590 K is shown in Fig. 5(a). Figure 5(b) shows calculated structure factors at 1000 K for different pressures. Extrapolation of the structure factors at 1000 K to $q = 0$ shows that there is a maximum phase separation tendency at around 40 GPa, which is consistent with the Gibbs free energy of mixing calculation.

C. Mixing and demixing behavior in Ca-Li alloy

We have also computed the partial pair correlation functions and Gibbs free energy of mixing for Ca-Li alloy to determine

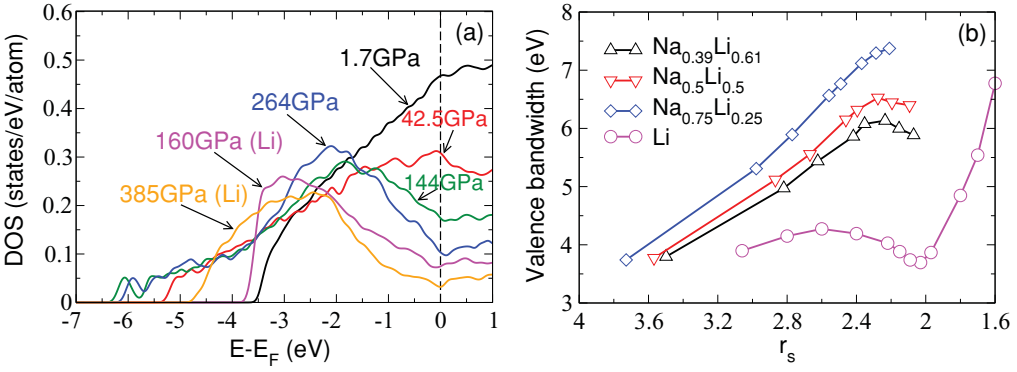

FIG. 7. (Color online) Electronic density of states (DOS) of $Na_{0.5}Li_{0.5}$ at 1000 K for various pressures. The DOS of pure Li at 160 and 385 GPa and 1000 K are also included. The Fermi level is taken as a reference. (b) Valence bandwidth of pure Li and Na-Li alloy as a function of r_s at 1000 K for different concentrations.

its mixing-demixing behavior at low and high pressure. The pair correlation functions at 3 and 267 GPa and 2000 K are shown in Figs. 6(a) and 6(b). At low pressure, the first-peak height of $g_{\mathrm{LiLi}}(r)$ is smaller than $g_{\mathrm{CaLi}}(r)$, while at high pressure the first-peak heights of $g_{\mathrm{CaCa}}(r)$ and $g_{\mathrm{LiLi}}(r)$ are larger than that of $g_{\mathrm{CaLi}}(r)$. This analysis is in agreement with the calculated negative and positive Gibbs free energies of mixing at low and high pressure. The Gibbs free energy of mixing (see Table I for the Gibbs free energies of pure Ca and Li and their mixture) at 3 and 267 GPa are found to be −72 and 115 meV, respectively. This indicates that the Ca-Li liquid alloy, which shows a mixing behavior at low pressure, phase separates at high pressure.

D. Electronic properties of Na-Li alloy

The electronic density of states of the $Na_{0.5}Li_{0.5}$ alloy at 1000 K for various pressures together with density of states of pure Li is shown in Fig. 7(a). The density of states at the Fermi level decreases with pressures and a dip near the Fermi level starts to develop at high pressure. A similar property is observed in pure Li.[4] Figure 7(b) shows the valence bandwidth as a function of r_s [where $\frac{4}{3}\pi(r_s a_0)^3 = V/N$, a_0 is the Bohr radius, V is the volume, and N is the number of atoms] for pure Li and Na-Li alloy at different concentrations. The valence bandwidth decreases at high pressure which is in agreement with reduction in coordination number shown in Fig. 4.

IV. CONCLUSION

In summary, we have implemented an efficient method to calculate the free energy and miscibility of liquid alloys using FPMD. The method can be used for computing melting curves as well. Thermodynamic data for Li, Na, Ca and their mixtures is provided, which may be useful for future studies of these systems. The mixing and demixing behavior of the alloys is also examined based on their structural properties. The computed electronic and structural properties of the Na-Li alloy, which phase separates, show that the Na and Li subsystems exhibit properties similar to the pure systems under pressure.

ACKNOWLEDGMENTS

This work is supported by ACEnet, LLNL, and NSERC. Work at LLNL is prepared under Contract No. DE-AC52-07NA27344. The authors would also like to thank ACEnet, LC, and WestGrid for providing computational facilities.

[1] V. E. Fortov, V. V. Yakushev, K. L. Kagan, I. V. Lomonosov, V. I. Postnov, T. I. Yakusheva, and A. N. Kuryanchik, JETP Lett. **74**, 418 (2001).
[2] M. Bastea and S. Bastea, Phys. Rev. B **65**, 193104 (2002).
[3] J. Y. Raty, E. Schwegler, and S. A. Bonev, Nature (London) **449**, 448 (2007).
[4] I. Tamblyn, J. Y. Raty, and S. A. Bonev, Phys. Rev. Lett. **101**, 075703 (2008).
[5] A. Yamane, F. Shimojo, and K. Hoshino, J. Phys. Soc. Jpn. **77**, 064603 (2008).
[6] A. Kietzmann, R. Redmer, M. P. Desjarlais, and T. R. Mattsson, Phys. Rev. Lett. **101**, 070401 (2008).
[7] A. M. Teweldeberhan and S. A. Bonev, Phys. Rev. B **78**, 140101(R) (2008).
[8] B. Rousseau and N. W. Ashcroft, Phys. Rev. Lett. **101**, 046407 (2008).
[9] J. Yang, J. S. Tse, and T. Iitaka, J. Phys. Condens. Matter **22**, 095503 (2010).
[10] H. Eshet, R. Z. Khaliullin, T. D. Kuhne, J. Behler, and M. Parrinello, Phys. Rev. B **81**, 184107 (2010).
[11] E. Gregoryanz, O. Degtyareva, M. Somayazulu, R. J. Hemley, and H.-K. Mao, Phys. Rev. Lett. **94**, 185502 (2005).
[12] E. R. Hernández and J. Íñiguez, Phys. Rev. Lett. **98**, 055501 (2007).
[13] L. Koči, R. Ahuja, L. Vitos, and U. Pinsook, Phys. Rev. B **77**, 132101 (2008).
[14] A. Lazicki, Y. W. Fei, and R. J. Hemley, Solid State Commun. **150**, 625 (2010).
[15] E. R. Hernández, A. Rodriguez-Prieto, A. Bergara, and D. Alfè, Phys. Rev. Lett. **104**, 185701 (2010).
[16] C. L. Guillaume *et al.*, Nature Physics, **7**, 211 (2011).
[17] C. J. Pickard and R. J. Needs, Phys. Rev. Lett. **102**, 146401 (2009).
[18] M. Canales, A. Giró, and J. À. Padró, J. Non-Cryst. Solids **205**, 907 (1996).
[19] Y. Senda, F. Shimojo, and K. Hoshino, J. Phys. Soc. Jpn. **67**, 2753 (1998).
[20] B. J. Costa Cabral and J. L. Martins, J. Chem. Phys. **111**, 5067 (1999).
[21] D. J. González, L. E. González, J. M. López, and M. J. Stott, Phys. Rev. E **69**, 031205 (2004).
[22] A. M. Teweldeberhan, J. L. Dubois, and S. A. Bonev, Phys. Rev. Lett. **105**, 235503 (2010).
[23] S.-T. Lin, M. Blanco, and W. A. Goddard III, J. Phys. Chem. B **119**, 11792 (2003).
[24] S.-T. Lin, P. K. Maiti, and W. A. Goddard III, J. Phys. Chem. B **114**, 8191 (2010).
[25] G. Kresse and J. Hafner, Phys. Rev. B **47**, 558 (1993).
[26] G. Kresse and J. Furthmüller, Phys. Rev. B **54**, 11169 (1996).
[27] P. E. Blöchl, Phys. Rev. B **50**, 17953 (1994).
[28] G. Kresse and D. Joubert, Phys. Rev. B **59**, 1758 (1999).
[29] Y. Wang and J. P. Perdew, Phys. Rev. B **44**, 13298 (1991).
[30] J. P. Perdew, J. A. Chevary, S. H. Vosko, K. A. Jackson, M. R. Pederson, D. J. Singh, and C. Fiolhais, Phys. Rev. B **46**, 6671 (1992).
[31] S. Nosé, J. Chem. Phys. **81**, 511 (1984).
[32] W. G. Hoover, Phys. Rev. A **31**, 1695 (1985).
[33] H. J. Monkhorst and J. D. Pack, Phys. Rev. B **13**, 5188 (1976).
[34] R. Hultgren, P. D. Desai, D. T. Hawkins, M. Gleiser, K. K. Kelley, and D. D. Wagman, *Selected Values of the Thermodynamic Properties of the Elements* (ASM, Metals Park, Ohio, 1973).
[35] H. Ruppersberg and W. Knoll, Z. Naturforsch. A**32**, 1374 (1977).